Synthesis and Characterization of Al-doped NiO Nanostructured Thin Films Elaborated by Solar Spray Pyrolysis Technique, for Photovoltaic Cells

Abdelbaki Nid [a,b,] *, Lilia Zighed [c], Yacine Aoun [d,e], Bedreddine Maaoui [d,e]

[a] *Mechanical Department, Faculty of Technology, University of Skikda, Skikda 21000, Algeria*
[b] *LGMM Laboratory, Faculty of Technology, University of Skikda, Skikda 21000, Algeria*
[c] *LGCES Laboratory, Faculty of Technology, University of Skikda, Skikda 21000, Algeria*
[d] *Mechanical Department, Faculty of Technology, University of El-Oued, El-Oued 39000, Algeria*
[e] *VTRS Laboratory, Faculty of Technology, University of El-Oued, El-Oued 39000, Algeria*
* *e-mail: ab.nid@univ-skikda.dz*

Abstract- In this experimental work, pure nickel oxide and Al-doped NiO thin films have successfully been elaborated onto glass substrates by solar spray pyrolysis technique. The substrates were heated at around 450°C using a solar heater (furnace). The structural, optical and electrical properties of the elaborated Al-doped films have been studied at different atomic percentage ratios (0, 0.5, 1, 1.5 and 2 at. %). The results of Al-doped NiO films XRD patterns were, the formation of (NiO) phase under a cubic crystalline structure (polycrystalline) with a strong favored orientation along (111) plane were noticed at all sprayed films. When Al doping ratio reaches 1 at.%, an growth in crystallite size over 31.9 nm was obtained denoting the nano-structure of the product, which confirmed by SEM images. In addition, aluminum oxide Al_2O_3 was clearly observed at 1.5 at.% Al ratio. Otherwise, all thin films have a good optical transmission in the visible region of about 65%, the optical band gap energy decreased from 3.69 to 3.64 eV with increasing Al doping ratio. It is shown that the layer deposited with 0.5 at.% has less disorder with few defects. The investigation on electrical properties of elaborated thin films confirmed that the conductivity of NiO films was improved, after doping them with Al which affirms their p-type character of semiconductor. However, an addition of an excessive quantity of Al content causes the formation of Al_2O_3 which leads to a decrease in the conductivity. It is worth mentioning that the Al content of 0.5 at.% is the optimum ratio in terms of electrical conductivity and formation defect. Al-doped NiO can be used in various optoelectronic devices due to its good transparency and high electrical conductivity.

Keywords: Nickel oxide; Thin films; Al doping ratio; Solar spray pyrolysis; Solar heater; Furnace.

1. INTRODUCTION

The recent research report that, the semiconductors as metallic oxides are essential compounds for the development of gas sensors, lithium ion micro-batteries, cathode materials for alkaline batteries, optoelectronics and ultrahigh frequencies components [1–2]. Among these, Nickel oxide (NiO) is a transparent p-type semiconducting material (TCO) has a direct large gap, and wide range of applications, such as gas sensors, UV photo-detector, dye-sensitized solar cells, electro-chromic coatings and counter electrodes layers of solid oxide fuel cells (SOFC) [3-4]. It has potential applications for solar cells is owing to its p-type character, gas sensors is due to its wide band gap (3.6-4.0eV), defrosting windows, transparent diodes and transistors because their transparency, it can be also used for

Preprints (www.preprints.org) | NOT PEER-REVIEWED | Posted: 30 November 2021 doi:10.20944/preprints202111.0572.v1

touch screens and UV photo-detectors because of their good responsively [5–6].

Nanostructure NiO thin films can be elaborated by several techniques such as sputtering, electron beam evaporation, molecular beam epitaxy, chemical vapor deposition, electro-deposition, spray pyrolysis and sol–gel process [7–8]. Among these processes, we will concentrate more particularly in this search on the spray pyrolysis, due to its various benefits such as inexpensive apparatus, wide homogeneous area, and easy control of the deposited films structure [9-10].

The aim of this search is to obtain Al-doped NiO thin films for optoelectronic applications, with a different heating way through using a solar heater (furnace) to economize the electrical energy and protect user from chemicals by working outside laboratories. The solar furnace (parabolic dish) consisted of a mirror layer inside (ITO glass) with parabolic reflector and a substrate holder at its focal point. It uses solar energy to heat a glass substrate fixed on the holder by reflecting the incident rays on it. The thin films can be deposited by spray pyrolysis (pneumatic) technique onto 450°C heated glass substrates with various doping ratios of 0.5, 1, 1.5 and 2 at. %. Investigation and characterization of structural and optical properties, of prepared thin films, were performed using X-ray diffraction, scanning electron microscope (SEM) and UV-visible spectroscopy. While for electrical properties, four-point probe were processed on all samples to correlate them to Al doping ratio.

2. EXPERIMENTS

Nickel (II) nitrate hexahydrate (Ni $(NO_3)_2.6H_2O$) was used to prepare NiO solution (0.1 M), and $AlCl_3.H_2O$ for Al_2O_3 solution. The solutions are mixed in volume equal volume of water. The Al contents are 0, 0.5, 1, 1.5 and 2 at.%, the mixture solution was stirred for 3 h at RT and heated at 50°C to yield a clear solution, in this setup drops of HCl can be added as a stabilizer with heating. After that, various Al doping ratios of NiO thin films were sprayed on 450°C preheated glass substrates by solar spray pneumatic method using solar furnace (see Figure 1a and 1b) for 5 minutes of deposition time. The obtained Al-doped NiO thin films have been characterized to identify the crystal structure, optical transmission and electrical conductivity by X-ray diffraction with an X-ray diffractometer (Bruker-AXS type 8D, with λ = 0.15406 nm and 2θ: 20–80°), Phenom ProX scanning electron microscope (SEM) an UV-visible spectrophotometer (Lambda 35 with wavelength range of 300–900 nm) and four-point method was performed by Keithley Model 2400-LV SourceMeter instrument, respectively.

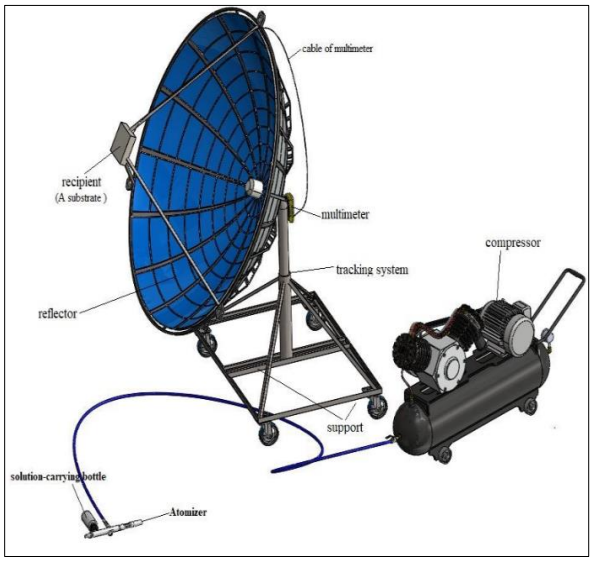

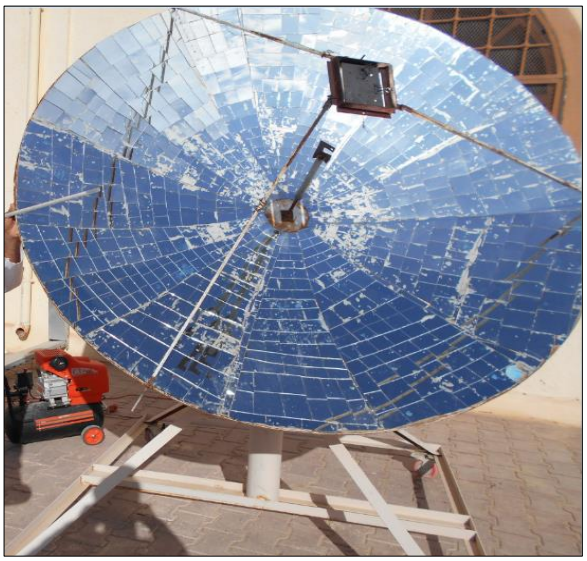

Figure 1. (a) Complete assembly of the experimental setup (Designed by SolidWorks)

(b) A picture of the used solar furnace

Preprints (www.preprints.org) | NOT PEER-REVIEWED | Posted: 30 November 2021 doi:10.20944/preprints202111.0572.v1

3. RESULTS AND DISCUSSION

Structural Properties of Al-doped NiO Thin Films

The effects of Al doping on crystal structure and favored orientations were studied by characterizing all sprayed Al-doped NiO thin films using the XRD technique. Figure 2 shows the XRD patterns of obtained thin films deposited with several Al doping ratios of 0, 0.5, 1, 1.5 and 2 at.%. As a first result, All films showed three diffraction peaks at 2θ = 37, 43 and 79° related to (111), (200) and (222) planes of NiO phase, denoting that NiO:Al thin films are polycrystalline (cubic structure), which is in a good accord with JCPDS data (card number 47-1049) [11]. The produced crystalline structures have strong peaks, corresponded to (111) crystal plane of the NiO face centered cubic (fcc) structure. It can be seen that the intensities of the (111) diffraction peaks of sprayed Al-doped NiO thin films compared to pure NiO film have good crystallinities, which affirmed the improvement of crystalline quality and reducing of crystal structure defects. The inset graph in Figure 2 shows the variations of diffraction angle and FWHM of the (111) diffraction. The smaller diffraction angle of the position peak was obtained for 1.5 at.%, indicating the increase in the interplanar spacing d_{111} (see Table1). However, the maximum value of the FWHM of the (111) peak measured for pure NiO film. The second result, it was observed at 2θ = 29.3° in the diffraction peak corresponding to appearance of a second phase getting clear at 0.15 at.% related to Al_2O_3 due to the abundance of O^{-2} outdoors, unlike inside laboratories.

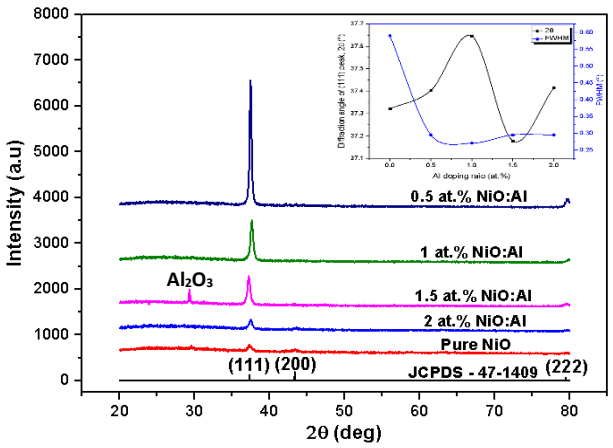

Figure 2: X-Ray diffraction spectra of NiO:Al thin films elaborated at 450°C with various Al doping ratio (at.%). The inset graph shows diffraction angle and FWHM variations of the (111) peak.

In order to get further structural information, several structural parameters of Al-doped NiO thin films elaborated with various Al doping ratio were calculated, such as interplanar spacing d_{hkl}, lattice constant *a*, grain size *G*, lattice strain ε, and dislocation density δ.

In the cubic structure case, the lattice constant *a* was calculated using the following formula (1) [12]:

$$\frac{1}{d_{hkl}^2} = \frac{h^2+k^2+l^2}{a^2} \quad (1)$$

Where *hkl* are Miller indices, and d_{hkl} is the interplanar spacing calculated by Bragg's law [13]:

$$2d_{hkl}\sin\theta = n\lambda \quad (2)$$

Where θ is the Bragg diffraction angle of peak in degree, *n* is the order of diffraction taken equal unity (first order), and λ is the wavelength of the incident radiation (λ = 1.5406 **Å**).

The crystallite size *G* of the films was calculated for (111) plane using Scherrer's formula [14-15]:

$$G = \frac{0.9\lambda}{\beta\cos\theta} \quad (3)$$

Where λ is the X-ray wavelength and β is the full width at half maximum (FWHM) corresponding to Bragg's diffraction angle θ.

The dislocation density δ, which is defined as the dislocation lines per unit volume of crystal, was calculated using the following formula [16]:

$$\delta = \frac{1}{G^2} \quad (4)$$

Table 1 sums up the structural parameters variations of elaborated Al-doped NiO thin films with various Al doping ratios. Crystallite size *G* and lattice strain ε variations along the (111) plane as a function of Al doping ratio are plotted in Figure 3.

It can be seen, the crystallite size increased to reach its maximum value of 31.9 nm at 1 at.% of Al, which maybe owing to the improvement of the crystalline quality. Whereas Al ratio exceeded 1 at.%, its size slightly decreased and fixed at 29.2 nm. At 1 at.%, the strain had a low value due to decreasing of lattice parameter [17].

The prepared film with Al content of 1 at.% presents the high value of crystallite size (31.9 nm) revealing the nanostructure of film. The increase in the crystallite size denotes a reducing in lattice defects, which in turn reduces dislocation density and strain (densely packed structure) [17] as shown in Table 1.

Preprints (www.preprints.org) | NOT PEER-REVIEWED | Posted: 30 November 2021 doi:10.20944/preprints202111.0572.v1

Table 1: Structural parameters deduced from the (111) peak of Al-doped NiO thin films with various Al doping ratios

Al doping ratio (at. %)	Diffraction angle 2θ (°)	FWHM β (°)	interplanar spacing d_{hkl} (Å)	Crystallite size G (nm)	Lattice parameter a (nm)	Lattice strain ε (%)	Dislocation density σ (lines/m²)
0	37.322	0.590	2.409	14.4	0.417	0.762	4.823
0.5	37.404	0.295	2.404	29.2	0.416	0.380	1.173
1	37.646	0.271	2.389	31.9	0.414	0.347	0.983
1.5	37.179	0.295	2.418	29.2	0.419	0.383	1.173
2	37.415	0.295	2.404	29.2	0.416	0.380	1.173

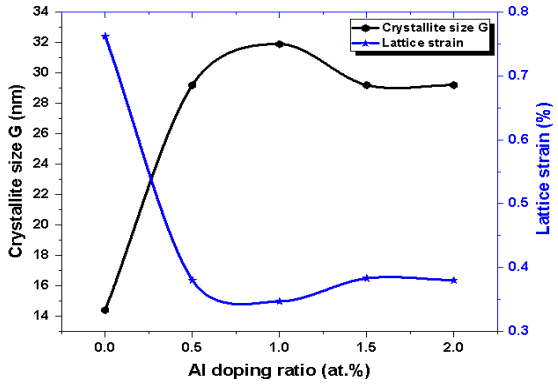

Figure 3: Crystallite size and lattice strain variations of NiO:Al thin films as a function of Al doping ratio.

Figures 4(a)–4(d) represent the SEM images of surface morphologies of the samples with different Al atomic percentage ratios (0.5, 1, 1.5 and 2 at. %). As can be seen, with increasing Al atomic percentage ratio to 1.5 at.%, the substrate becomes well covered with presence of nanoagglomerations along the surface of the substrate as seen in Figure 3(c). Beyond 1.5 at.% as Al atomic percentage, the substrate becomes completely covered with NiO and films exhibing that nanoagglomerations continue its formation to becoming microagglomerations; figure 4(d).

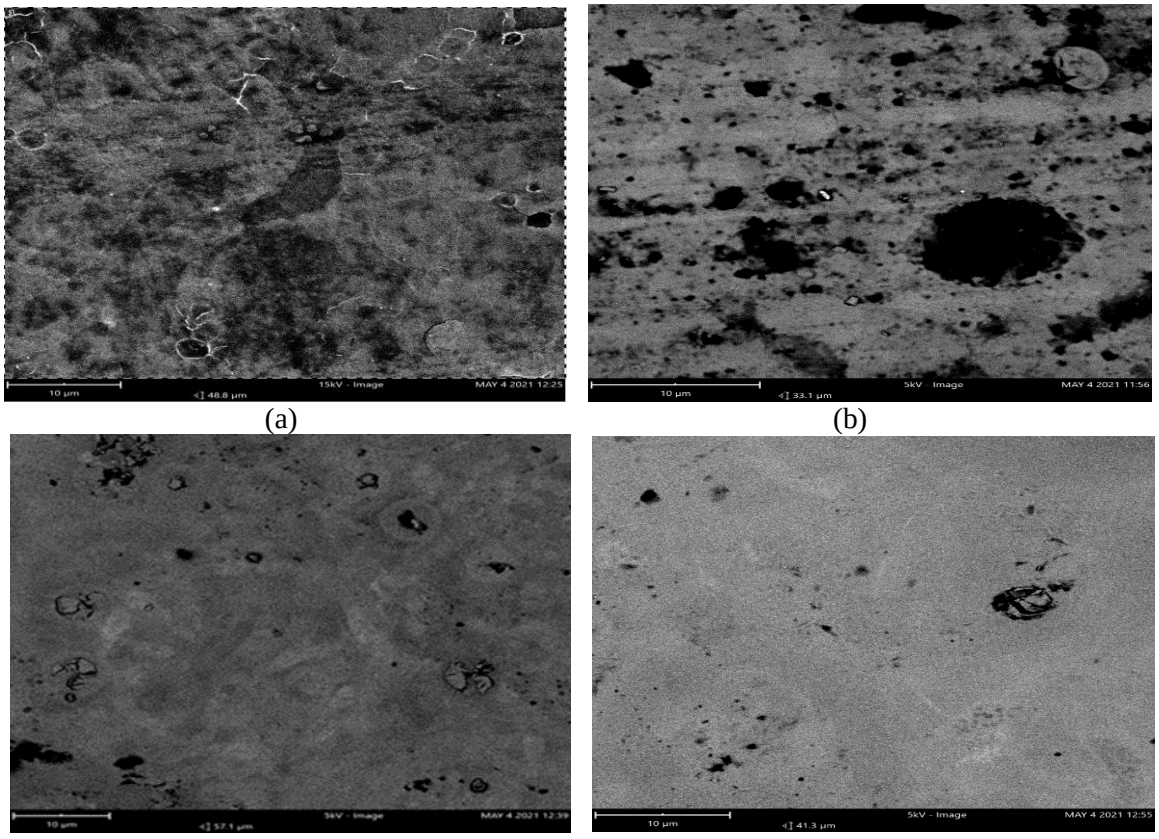

(a) (b) (c) (d)

Figure 4: SEM Images of Al-doped NiO thin films prepared at 450°C with different Al atomic percentage ratios, (a) samples prepared with 0.5, (b) with 1.0, (c) with 1.5, and (d) with 2 at %.

Preprints (www.preprints.org) | NOT PEER-REVIEWED | Posted: 30 November 2021 doi:10.20944/preprints202111.0572.v1

Optical Properties of Al-doped NiO Thin Films

To determine optical properties of the deposited Al-doped NiO thin films versus Al doping ratios, transmittance spectra were measured. The obtained results are shown in Figure 5.
We observe from this figure that, transmission decreases with increasing Al doping ratio in NiO thin films.

For all Al-doped NiO films elaborated with different Al doping ratios, spectra appear two ranges: the first one at wavelengths greater than 400 nm appearing practically an average transmission between 53 and 76% and revealing a decrease with increasing Al doping ratio and, based on calculated film thickness (d), transparence was depending on thickness of samples revealing Beer-Lambert's law as shown in Table 2. The second range is at wavelengths lower than 400 nm for which transparence decreases speedily for all films exhibiting the beginning of fundamental absorption owing to the transition between the conduction and the valence bands [18].

The calculation of the optical band gap can be playing an essential role to characterize the thin film, which based on optical transmission. It was estimated (calculated) from the classical method by using of the curve at $A = 0$ [19], which represented to the drawn of $(A\upsilon)^2$ as a function of $h\upsilon$ (see Figure 6) using the following formulas [2-5]:

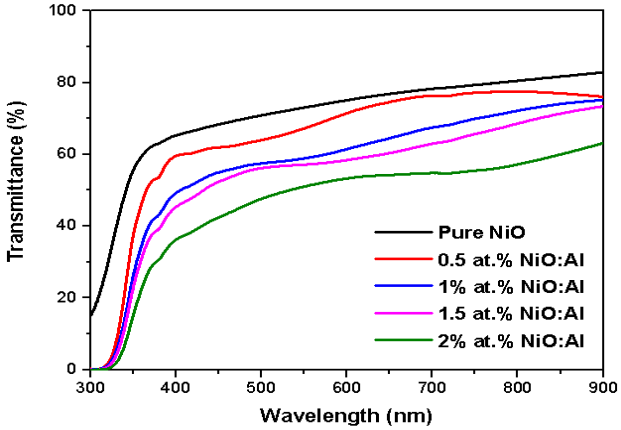

Figure 5: Spectral transmittance curves of NiO:Al thin films with various Al doping ratios.

$$A = \alpha\, d = -\ln T \quad (5)$$

$$(A\upsilon)^2 = C\,(h\upsilon - E_g) \quad (6)$$

Where A is the absorbance, d is the film thickness; T is the transmission spectra; α is the absorption coefficient values; C is a constant, $h\upsilon$ is the photon energy and E_g the band gap energy of thin films.
On the other hand, the disorder in the thin films was characterized by Urbach energy (E_u) which has been calculated by the following equation [20]:

$$A = A_0 \exp^{\left(\frac{h\upsilon}{E_u}\right)} \quad (7)$$

Where A_0 is a constant and $h\upsilon$ is the photon energy.
Figure 7 shows LnA variation versus photon energy $h\upsilon$ for films. Eu values were calculated from reciprocal slopes of the straight lines, as shown in the Figure 7.

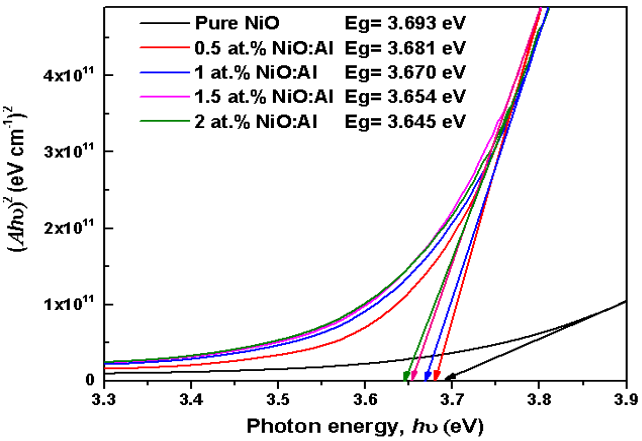

Figure 6: $(A\upsilon)^2$ variation versus $h\upsilon$ of each NiO:Al thin film to estimate band gap energy Eg.

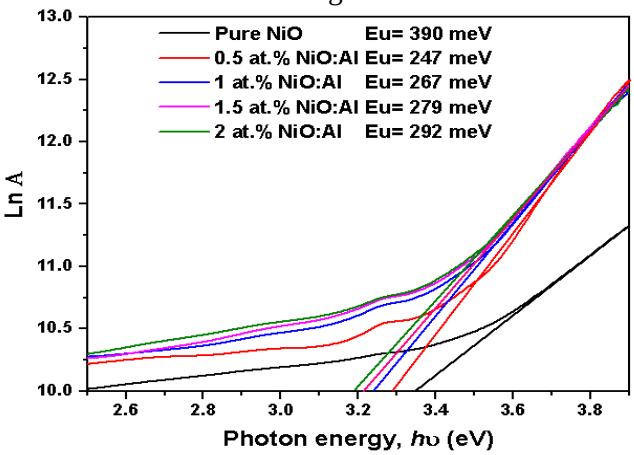

Figure 7: LnA variation versus $h\upsilon$ of each NiO:Al thin film to estimate Eu.

Preprints (www.preprints.org) | NOT PEER-REVIEWED | Posted: 30 November 2021 doi:10.20944/preprints202111.0572.v1

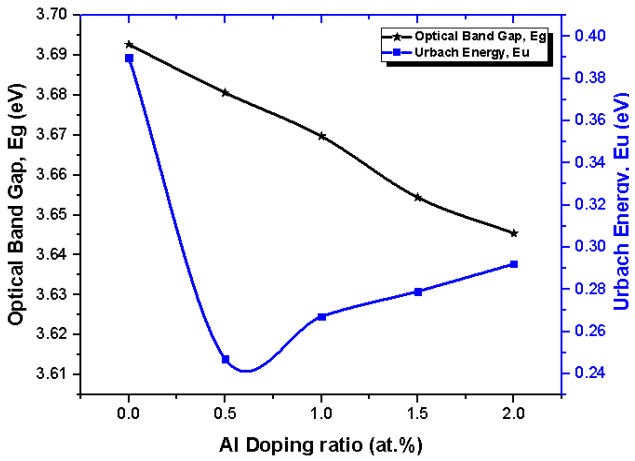

Figure 8: Optical band gap E_g vs. Urbach energy E_u of NiO:Al films as a function of Al doping ratio.

Figure 8 shows the inverse trends of optical band gaps and Urbach energies calculated for doped thin films, the variables are listed in Table 2. As can be seen from this table, the energy band gap is between 3.64–3.70eV which is in good accord with the Eg values of bulk NiO (3.6-4 eV) [21] and results carried out in literature [22]. The decrease in the optical band gap with increasing Al doping ratio in NiO may be attributed to the free carriers' effect as well as to impurity effects on the band gap [23].

The highly decrease of the Urbach energy by 30% from for Al-doped NiO films compared to pure NiO film, can be explained by increasing of crystallite size to 29.2 - 31.9 nm and decreasing of the strain.

Table 2: Values of thickness *d*, average transmittance, band gap energy E_g, Urbach energy E_u and electrical conductivity σ of Al-doped NiO thin films prepared at 450°C with various Al doping ratios.

Al doping ratio (at.%)	Thickness d (nm)	Average transmittance (%)	Gap energy Eg (eV)	Urbach energy Eu (eV)	Electrical conductivity σ $(Ohm.cm)^{-1}$
0	154.550	71.205	3.693	0.390	0.032
0.5	163.847	64.683	3.681	0.247	0.641
1	191.296	57.529	3.670	0.267	0.228
1.5	202.103	54.550	3.654	0.279	0.234
2	252.289	46.416	3.645	0.292	0.098

Preprints (www.preprints.org) | NOT PEER-REVIEWED | Posted: 30 November 2021 doi:10.20944/preprints202111.0572.v1

Electrical Properties of Al-doped NiO Thin Films

The four-point probes method was used to calculate the electrical conductivity σ of Al-doped NiO films; the measurement was based on the sheet resistance R_{sh}. It is obtained by the following expression [24]:

$$\sigma = \frac{1}{R_{sh}d} = \left(\frac{\pi}{\ln(2)}\frac{V}{I}\right)^{-1} \quad (8)$$

Where I is the applied current = $0.5.10^{-6}$A and V is the measured voltage and d is the film thickness. Figure 9 shows the electrical conductivity and Urbach energy of Al-doped NiO films plotted as function of different Al doping ratio. As can see from this plot, the electrical conductivity increased up to maximum value 0.641 $(\Omega.cm)^{-1}$ obtained with Al ratio of 0.5 at.%, then decreased by increasing Al ratio to reach 0.098 $(\Omega.cm)^{-1}$ at 2 at.%. As a result of the compositional changes, especially in terms of the formation and occupation of nickel vacancies (defect), these lead to p-type conductivity.

As the ionic radii of Al^{+3} and Ni^{+3} ions are very close, by introducing Al^{+3} ions as the dopant in the NiO film, it may easily replace the Ni^{+3} ions or occupy interstitial sites of NiO matrix [23-25]. However, an addition of an excessive Al quantity may cause the formation of Al_2O_3 and related groups as carrier traps contrary to electron donors, resulting in a decrease in the conductivity and other associated phenomena, that what happened when Al doping ratio exceed 0.5 at.% .

Figure 8 supports this analysis, the variations of electrical conductivity and Urbach energy are revealing an inverse behavior which means that doping of NiO by Al leads to decrease the formation defects of NiO matrix which appears through the decreasing of Urbach energy and increasing of electrical conductivity in doped films.

It is worth noting that the electrical conductivity (σ) of the elaborated Al-NiO films, have p-type character, and the highest electrical conductivity achieved was $0.641(\Omega.cm)^{-1}$ at 0.5 at.%, with lowest Eu, 0.247 eV.

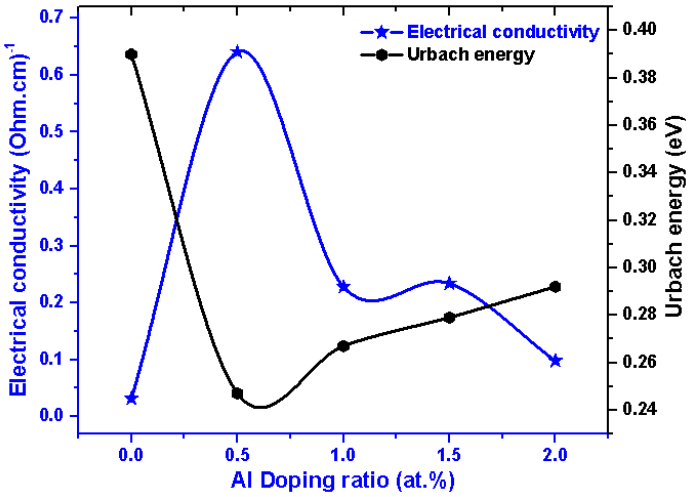

Figure 9: Electrical conductivity σ vs. Urbach energy E_u of NiO:Al films with different Al doping ratio.

4. CONCLUSION

In the end, Al-doped NiO thin films have successfully been elaborated onto glass substrates by solar spray pneumatic method, at around 450°C with a different heating way by using a solar furnace. The effect Al doping ratio (0, 0.5, 1, 1.5 and 2 at.%) on structural, optical and electrical properties was investigated. The followings conclusions summarize the above research work:

(1) XRD patterns of Al-doped NiO thin films indicate that the obtaining thin films are poly-crystalline with a face centered cubic structure (fcc) and a strong (111) favored orientation for all sprayed films. The structure was improved for doped thin films, the crystallite size increased up to maximum value of 31.9 nm for sprayed film with 1 at.% Al which revealing the nano-structure of the product. SEM images reveal that with increasing Al atomic percentage ratio, the substrates become better covered and confirm the formation of homogeneous nanostructured films. However, aluminum oxide Al_2O_3 was observed when Al content exceeded 0.5 at.%.

(2) All Al-doped NiO thin films have good transmission in visible region of about 65%. When the Al doping ratio increased from 0 to 2

at.%, a band gap shrinkage of up to 0.048 eV was observed. It is also shown that the doped films by Al have low values of Urbach energy, the minimum value reached was, 0.247 eV at 0.5 at.% Al which is the film has less disorder and few defects.

(3) The electrical conductivity of the elaborated Al-doped NiO thin films increased greatly from 0.03 $(\Omega.cm)^{-1}$ for undoped NiO film to 0.1 – 0.64 $(\Omega.cm)^{-1}$ for Al-doped NiO films due to composition changes after aluminum ions incorporation in NiO matrix. However, an addition of an excessive Al quantity (exceed 0.5 at.%) causes the formation of Al_2O_3 which resulting a decrease in the conductivity. It can be noted that the conductivity of films have p-type (semiconductor) character.

The good transmittance, widened band gap (3.64–3.70eV) and high electrical conductivity (0.64 $(\Omega.cm)^{-1}$) obtained for Al-doped NiO films make them promising candidate for electronic and optoelectronic applications such as photo-detectors (diodes, transistors...) and solar cells.

REFERENCES

[1] Y.Aoun, R.Meneceur, S.Benramache, B.Maaoui, *Sprayed NiO-Doped p-Type Transparent ZnO Thin Films Suitable for Gas-Sensing Devices, Physics of the Solid State* 62 (1) 131– 136 (2020).

[2] H.Guezzoun, B.Benhaoua, S.Benramache, *Synthesis and characterizations of nanocrystalline Na and Al codoped NiO thin films, International Journal of Integrated Engineering* 12 (1) 204-209 (2020).

[3] Z.W.Shang, H.H.Hsu, Z.W.Zheng, C.H.Cheng, *Progress and challenges in p-type oxide-based thin film transistors, Nanotechnology Reviews* 8, 422–443 (2019).

[4] Mironova-Ulmane N., Kuzmin A., Sildos I., Puust L., Grabis J., Magnon and *Phonon Excitations in Nanosized NiO*, Latvian Journal of Physics and Technical Sciences 56, 726–737 (2019).

[5] F.J. Garcia-Garcia, P. Salazar, F. Yubero, A.R. González-Elipe, *Non-enzymatic glucose electrochemical sensor made of porous NiO thin films prepared by reactive magnetron sputtering at oblique angles, Electrochimica Acta* 20138–44 (2016).

[6] G.S. Gund, C.D. Lokhande, H.S. Park, *Controlled synthesis of hierarchical nanoflake structure of NiO thin film for supercapacitor application, Journal of Alloys and Compounds* 741, 549-556 (2018).

[7] I.Manouchehri, D.Mehrparvar, R.Moradian, K.Gholami, T.Osati, *Investigation of structural and optical properties of copper doped NiO thin films deposited by RF magnetron reactive sputtering, Optik* 127 8124–8129 (2016).

[8] M. Karyaouia, D. Ben Jemiaa, M. Gannounia, I. Ben Assakera, A. Bardaouia, M. Amloukb, R. Chtouroua, *Characterization of Ag-doped ZnO thin films by spray pyrolysis and its using in enhanced photoelectrochemical performances, Inorganic Chemistry Communications* 119, 108114 (2020).

[9] Yahya M. Abdul-Hussein, Huda J. Ali, L. A. Latif, Mudar Ahmed Abdulsattar, Husham M. Fadhel. *Preparation of Al-doped NiO thin films by spray pyrolysis technique for CO gas sensing. J Adv Pharm Edu Res*; 9(3):1-6 (2019).

[10] F. A. Garces, N. Budini, J. A. Schmidt, and R. D. Arce, *Highly doped ZnO films deposited by spray-pyrolysis. Design parameters for optoelectronic applications, Thin Solid Films*, vol. 605, pp. 149–156, (2016).

[11] J. Wang, P. Yang, X. Wei, and Z. Zhou, *Preparation of NiO two-dimensional grainy films and their high-performance gas sensors for ammonia detection, Nanoscale Research Letters*, vol. 10, no. 1, pp. 1–6, (2015).

[12] H.-L. Chen, Y.-M. Lu, and W.-S. Hwang, *Effect of film thickness on structural and electrical properties of sputter-deposited nickel oxide films, Materials Transactions*, vol. 46, no. 4, pp. 872–879, (2005).

[13] B. Cullity and S. Stock, *Principles of X-Ray Diffraction, Addison Wesley*, Mass, USA, (1978).

[14] A.Diha, S.Benramache, L.Fellah, *the Crystalline Structure, Optical and*

Conductivity Properties of Fluorine Doped ZnO Nanoparticles, *Journal of Nano and Electronic Physics* 11 03002 (2019).

[15] Y.Yulizar, R.Bakri, D.Oky B.Apriandanu, T.Hidayat, *ZnO/CuO nanocomposite prepared in one-pot green synthesis using seed bark extract of Theobroma cacao*, *Nano-Structures & Nano-Objects* 16 300–305 (2018).

[16] A.G. Habtea, F.G. Honea, F.B. Dejene, *The influence of malonic acid on the structural, morphological and optical properties of CdSe thin films prepared by chemical bath deposition method*, *Inorganic Chemistry Communications* 103 107-112 (2019).

[17] N. Khedmi, M. Ben Rabeh, and M. Kanzari, *Structural morphological and optical properties of $SnSb_2S_4$ thin films grown by vacuum evaporation method*, *Journal of Materials Science and Technology*, vol. 30, no. 10, pp. 1006–1011 (2014).

[18] S. Benramache and B. Benhaoua, *Influence of substrate temperature and Cobalt concentration on structural and optical properties of ZnO thin films prepared by Ultrasonic spray technique*, *Superlattices and Microstructures*, vol. 52, no. 4, pp. 807–815, (2012).

[19] Y.Aoun, M.Marrakchi, S.Benramache, B.Benhaoua, S.Lakel, A.Cheraf, *Preparation and Characterizations of Monocrystalline Na Doped NiO Thin Films*, *Materials Research* 21 e20170681 (2018).

[20] S. Benramache, Y. Aoun, S. Lakel, H. Mourghade, R. Gacem, B. Benhaoua, *Effect of Annealing Temperature on Structural, Optical and Electrical Properties of ZnO Thin Films Prepared by Sol-Gel Method*, *Journal of Nano- and Electronic Physics* 10 No 6, 06032 (2018).

[21] S.A. Mahmoud, S.Alshomer, M.A.Tarawnh, *Structural and optical dispersion characterisation of sprayed nickel oxide thin films*, *Journal of Modern Physics* 2 1178-1186 (2011).

[22] B. Maaoui, Y. Aoun, S. Benramache, A. Nid, R. Far, A. Touati, *Synthesis and characterization of physical properties of the NiO thin films by various concentrations*, *advances in materials science*, Vol. 20, No. 3 (65), (2020).

[23] S Nandy, U N Maiti, C K Ghosh1 and K K Chattopadhyay, *Enhanced p-type conductivity and band gap narrowing in heavily Al doped NiO thin films deposited by RF magnetron sputtering*, *J. Phys.: Condens. Matter* 21 115804 (2009).

[24] Y.Aoun, *Design and development of the solar oven for the preparation of metal oxides-oxides characterization*, *Doctoral thesis*, Mohamed khider University, Algeria (2016).

[25] Rajeh M. Mundle, Hampton S. Terry, Kevin Santiago, Dante Shaw, Messaoud Bahoura, Aswini K. Pradhan, Kiran Dasari, and Ratnakar Palai , *Electrical conductivity and photoresistance of atomic layer deposited Al-doped ZnO films*, *J. Vac. Sci. Technol.* A, Vol. 31, No. 1, (2013).